Topology Optimization and Freeform Fabrication Framework for Developing Prosthetic Feet

Nicholas P. Fey, Brian J. South, Carolyn C. Seepersad, Richard R. Neptune

Department of Mechanical Engineering, The University of Texas at Austin

Abstract

The ability to easily design and manufacture prosthetic feet with novel design characteristics has great potential to improve amputee rehabilitation and care. This study presents a framework using topology optimization methods to develop new prosthetic feet to be manufactured using selective laser sintering. As an example application, the framework was used to generate a prosthetic foot that minimizes material usage while trying to replicate the stiffness characteristics of a commercially available carbon fiber foot. The solution was validated using finite element methods to verify the foot's loading response, and a prototype was manufactured. The result was a novel foot design that with future design modification has the potential to improve amputee gait by providing energy storage and return and reducing prosthetic weight.

Introduction

A recent study estimated that in 2005 approximately 1.6 million persons in the U.S. were living with limb loss (~40% major lower limb amputations) and that this total will more than double to 3.6 million by 2050 [1]. A wide range of demands are placed upon the prosthetic feet worn by amputees ranging from normal and fast walking to running and participation in recreational activities [2]. Therefore, the proper choice of foot is critical to reduce the negative effects of limb loss that include: temporal and ground reaction force asymmetry [3-6], higher metabolic cost [7], increased prevalence of intact knee osteoarthritis [8, 9], asymmetric joint loading [6, 10-14], altered residual leg muscle activation patterns [15-17], chronic leg and back pain [8, 18-20] and reduced walking speed [11, 21-23]. Traditionally, most prosthetic feet have been solid ankle cushioned heel (SACH) designs (Fig. 1A) that reduce contact forces during the initial loading response following heel-strike, but provide minimal energy return during late stance. Recently, increased use of carbon fiber, a high-strength and lightweight composite, has facilitated prosthetic designs to be energy storage and return (ESAR) feet, which attempt to replace lost function of the ankle plantar flexors and improve amputee walking by storing elastic energy throughout stance and releasing it during late-stance to provide forward propulsion and swing initiation [24-26]. Due to the higher strength to weight ratio of carbon fiber, several designs are currently available for patient prescription (Fig. 1B).
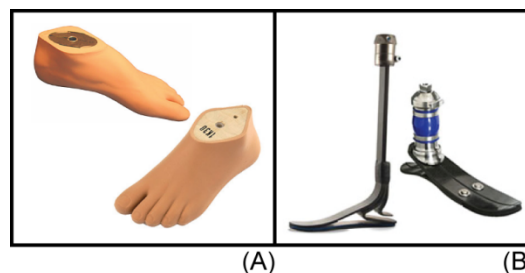

(A)   (B)

Figure 1. Two commercially-available SACH feet (A) and two ESAR feet (B). Images URL: www.extremeprosthetics.com/finnieston_feet.htm, http://www.ottobock.com/cps/rde/xchg/ob_com_en/hs.xsl/7212.html, http://medexinternational.com/htm/prost/sachfeet.htm

Selective laser sintering (SLS) technology has been used to effectively produce ankle-foot orthoses and below-knee prosthetic sockets [27-31]. Due to the small number of manufacturing constraints using SLS, an optimization approach is ideal to produce and investigate novel prosthetic designs. Previous studies have used topology optimization techniques on a variety of tasks to optimize the layout of a product or component (cf. [33-35]). In biomechanics related applications, they have been implemented to generate implant scaffold designs [36], simulate bone morphology and growth [37], and to design compliant features in amputee prosthetic sockets [27]. However, their application to produce new, unconventional prosthetic foot designs remains unexplored. Therefore, coupling topology optimization design methods with SLS manufacturing may serve as a more effective way to produce novel prosthetic feet compared to the commonly used carbon fiber technology. The goal of this study was to develop a framework that uses topology optimization techniques to produce novel prosthetic feet well-suited for SLS fabrication and to validate its use by creating a foot that replicates stiffness characteristics of a commercially available ESAR foot and minimizes material usage.

Methods

The commercially available Highlander (FS 3000) from Freedom Innovations, Inc. (Fig. 2A), a commonly-prescribed, carbon fiber ESAR foot, was chosen as a target for replication of stiffness characteristics. In a previous study, the loading response of this foot was replicated with a foot fabricated with SLS technology [38]. However, this SLS ESAR foot (Fig. 2B) [38] was designed to maintain the same sagittal plane geometry of the original carbon fiber foot, and new topologies were not explored. The previous design was modeled and tested by finite element methods (FEM), validated experimentally through compression testing, and used in a case study on a below-knee amputee walking at 1.2 m/s. In the present study, the final design is generated with topology optimization techniques, compared to the carbon fiber design shape, and then validated with FEM in comparison to the solid model of the SLS ESAR foot with respect to material usage and loading response. A comparison of the material usage objective during FEM validation would not have been valid if a solid model of the carbon fiber foot had been used because of the different materials (carbon fiber and Nylon-11).
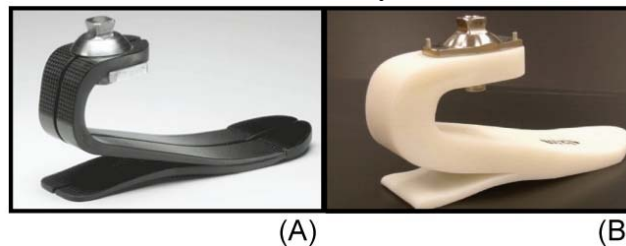

(A)   (B)

Figure 2. The Highlander (FS 3000, A), available from Freedom Innovations, Inc. was used to test the topology optimization framework. URL: http://www.freedom-innovations.com. A solid model of the SLS ESAR foot (B) made from Nylon-11 that replicated the loading response of the carbon fiber Highlander (FS 3000) [38] was used for comparison during FEM validation.

Topology Optimization

The topology optimization design space consisted of a two-dimensional grid of square planar finite elements (Fig. 3) that represented the sagittal plane. The design variables in the optimization problem were the density of each element (2448 elements total).
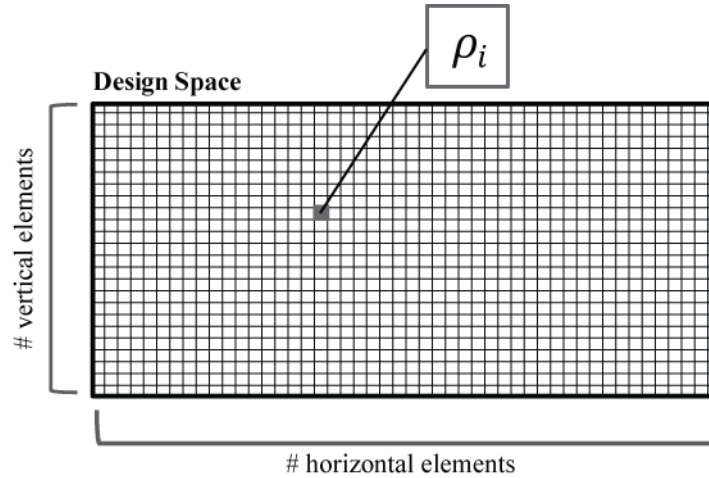
Figure 3. Theoretical topology optimization grid consisting of a finite set of square planar finite elements, with each element density (ρ_i) representing a design variable. The constructed design space used in this study was 34 vertical elements by 72 horizontal elements.

A topology optimization program [39] was modified and executed in MATLAB (MathWorks, Inc.). The program used a solid isotropic microstructure with penalization (SIMP) technique, also known as the artificial material model. The SIMP finite element formulation defined compliance as a measure of strain energy stored in a structure under a given set of loading conditions (Eq. 1). Each element was represented by four nodes and was linear in a plain-strain finite element formulation. The density of each element affected its local stiffness (Eq. 1).

$$c(\rho_i) = U^T K U = \sum_{i=1}^{N} u^T k_i u \, , \quad c = compliance$$
$$k_i = \rho_i{}^p E$$
$$p \geq 1.0$$
$$0.001 \leq \rho_i \leq 1.0 \tag{1}$$

Global displacement (U) and stiffness (K) matrices were defined in terms of the element displacement vector (u) and element stiffness matrix (k_i), respectively [39]. The local stiffness matrix for each element (k_i) was defined in terms of elastic modulus (E), element density (ρ_i), and constant (p) that penalizes intermediate element density values between fully-dense ($\rho_i \cong 1.0$) and void ($\rho_i \cong 0.001$) elements. The total number of elements (N) was calculated as the product of the number of horizontal and vertical elements (Fig. 3) [39]. A modulus conversion was needed to properly compare the compliance values between the nominal carbon fiber design (Fig. 3) and topology optimization solutions. The shape input for the nominal design was based on a carbon fiber foot, while this framework's goal was to produce feet suitable for SLS fabrication. Thus, a conversion was made to convert between carbon fiber (E=300 GPa) and Nylon-11 (E=1.4 GPa) materials to compare compliances [30, 41].

The topology optimization program [39] utilized a method of moving asymptotes (MMA) algorithm [40] for optimization. The MMA subroutine yielded a new design solution using the

current design solution, problem constraints and minimization objectives. MMA is ideal in this design problem because of a large number of design variables (density of each element) and the ability to use inequality constraints. Also, MMA required the objective and constraint functions with the derivatives of these two with respect to a given design variable. In the optimization problem, volume and compliance were expressed explicitly in terms of element density (Eqs. 1 and 2) [39].

$$V = \sum_{i=1}^{N} \rho_i , \qquad V = volume \qquad\qquad (2)$$

The sagittal plane cross-sectional geometry of the carbon fiber prosthetic foot was discretized by tracing the shape of the nominal carbon fiber foot on graph paper and input into the topology optimization design space (Figs. 4A, 4B).
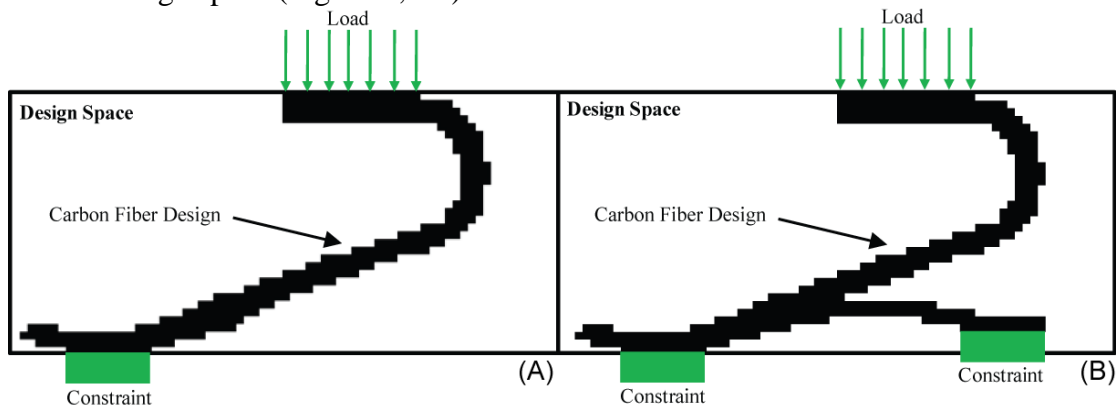

Figure 4. Nominal carbon fiber foot geometry of the keel (A) in the toe-only loading condition, and keel and heel (B) in the foot flat loading condition. The nodes at the bottom of the keel and heel sections were constrained to translate only in the horizontal direction, representing contact with the ground.

The compliance of the carbon fiber design's keel section was evaluated in a toe-only loading condition, and the compliance of the keel and heel sections together was evaluated in a foot-flat loading condition. These two compliance values served as targets for new designs. For the toe-only and foot-flat conditions, a distributed load (Figs. 4A, 4B) was applied to the nodes on the top portion of the foot. The nodes on the bottom portion of the foot were constrained to move only in the horizontal direction, representing contact with the ground (Figs. 4A, 4B). The keel section of ESAR feet is important for storing energy during the stance phase of gait to be released at toe-off, and the heel section reduces contact forces during the initial loading response following heel-strike. Thus, topology optimization was broken into two parts. First, the optimization algorithm solved for keel section geometry by minimizing volume and attempting to match the compliance of the keel section of the nominal carbon fiber foot in a toe-only loading condition. Then, the previously-optimized geometry of the keel section was fixed, and the shape of the heel section was optimized to minimize volume and match the carbon fiber compliance in a foot-flat loading condition. In both instances of optimizing the keel and heel geometries, the design problem was formulated in the same manner.

Problem Formulation

Find:
$\rho_i = element\ densities$

Minimize:
$$Cost(\rho_i) = \frac{\left|c(\rho_i) - c\left(\rho_{i,carbon\ fiber}\right)\right|}{c\left(\rho_{i,carbon\ fiber}\right)} + \frac{\sum_{i=1}^{N} \rho_i}{\sum_{i=1}^{N} \rho_{i,carbon\ fiber}}$$

$\rho_{i,carbon\ fiber} = element\ density\ of\ the\ carbon\ fiber\ design\ (Figs.\ 4A, 4B)$

With constants:
$\#\ vertical\ elements = 34$
$\#\ horizontal\ elements = 72$
$p = 3.0$

Subject to the constraints:
$0.001 \leq \rho \leq 1.0$

$$V = \sum_{i=1}^{N} \rho_i \leq \sum_{i=1}^{N} \rho_{i,carbon\ fiber}$$

The compliance and volume objectives were normalized by the compliance and volume of the carbon fiber design, respectively. All initial element densities were set to $\rho_i = 0.5$. Convergence time varied and were all less than 1 minute.

The influence of allowable design space on the solutions generated via topology optimization was explored by implementing a series of geometric constraints, as described in the subsequent results section. This was done to ensure the final solution generated would fit within a cosmetic foot cover and shoe. These geometric constraints were implemented by setting the element densities (ρ_i) of voided sections to 0.001 (~0) before every function call of the MMA subroutine. Similarly, the top region of the final solution was constrained to be filled ($\rho_i = 1.0$) to allow for proper attachment to the pylon and socket assembly in the future.

Solid Model Creation and Finite Element Method (FEM) Validation
The final topology optimization solution was validated using computer-aided design (CAD) modeling in SolidWorks and FEM compression tests using COSMOSWorks (SolidWorks, Inc.). The FEM response of the final solution CAD model was compared to the response of the SLS ESAR foot model that, following its fabrication from Nylon-11, replicated the loading response of the nominal carbon fiber design (Fig. 2B) [38]. 3D parabolic tetrahedral solid elements with four corner nodes and six side nodes were used. Element size was generated automatically to ensure a smooth surface. A compression simulation assembly was created in which immovable plates were placed to contact the bottom surface of the feet (representing the ground) and a loading block was placed at the top of the foot which applied the given load [38]. Loads applied were 113 and 34 kg for foot-flat and toe-only, respectively. FEM comparisons were made in both

the toe-only and foot-flat loading conditions [38] to ensure the maximum stress reached did not exceed the yield strength of Nylon-11 and to compare displacements of the solution with the SLS ESAR foot in these conditions. Lastly, a prototype was manufactured of the final solution from Nylon-11 (Rilsan D80) in a 3D Systems HiQ SLS machine to verify its production using SLS fabrication.

Results

Topology Optimization – Toe-Only Loading Condition

A series of successive geometric constraints to the allowable design space (Figs. 5A-5D) were made beginning with an unconstrained design space (Fig. 5A) and evolving to a design space that ensured the final design would fit within a cosmetic foot cover and shoe. The initial keel section solution (Fig. 5E) generated using the original design space (Fig. 5A) was not a practical solution that would fit within a cosmetic foot cover. Thus, constraints (Figs. 5B-5D) were imposed such that the solutions (Figs. 5F-5H) were not allowed to occupy voided regions and would ultimately fit within a cosmetic foot cover (Figs. 5G, 5H). The outer bounds for the solution (Fig. 5C) were determined by tracing the shape of a cosmetic cover on the same graph paper used previously. Furthermore, the voided design space was expanded (Fig. 5D) to eliminate the possibility of a single vertical member (Fig. 5G), which would perform poorly due to anterior-posterior loads placed on the foot during gait. The final keel section solution (Fig. 5H) took on a similar shape to the nominal carbon fiber and SLS ESAR designs, but with a truss-like structure. Also, the top region of the final solution was constrained to be filled ($\rho_i = 1.0$) to allow for proper attachment to the pylon and socket assembly. The single point of contact between the upper and lower section of the keel section was noted as a possible stress concentration. However, the next step using topology optimization solved for the heel section geometry, which added additional material to this area of concern and alleviated the potential weakness.
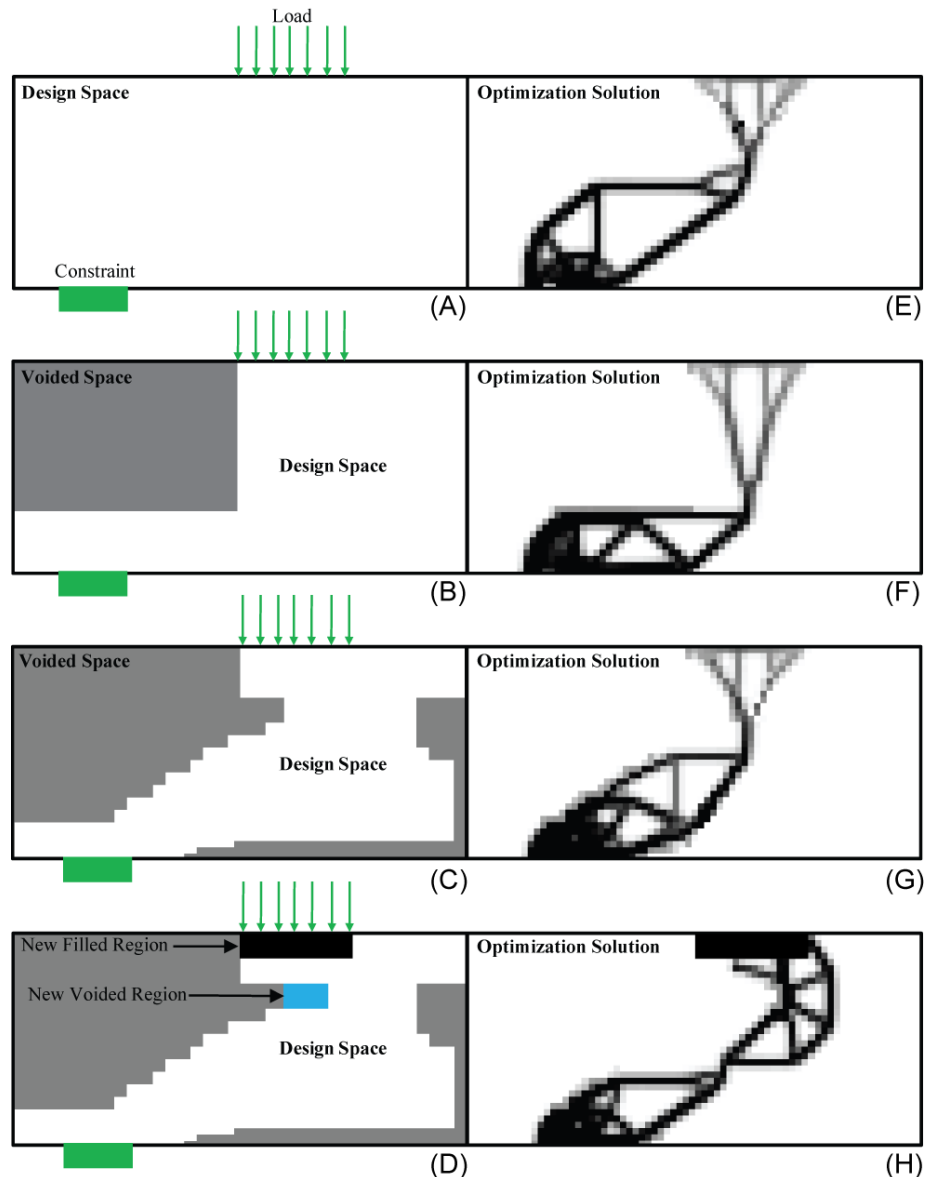
Figure 5. Successive geometric constraints imposed on the allowable design space (A-D) with their respective topology optimization solutions for the keel section geometry (E-H). A vertical distributed load was applied to the nodes along the top of the foot. The nodes at the bottom of the keel section were only allowed to translate in the horizontal direction, which represented ground contact.

Topology Optimization – Foot-Flat Loading Condition

The final keel solution (Fig. 5H) from the toe-only loading condition was fixed while the topology optimization created the heel section based on the remaining design space. The optimization attempted to replicate the compliance of the carbon fiber shape in a foot-flat loading condition and minimize volume. The initial heel design (Fig. 6C) consisted of a vertical support member to direct loading to the ground. The heel solution was not a practical shape and would not perform well due to the experienced anterior-posterior ground reaction forces during gait. Therefore, the design space was further constrained (Fig. 6B). The final topology optimization

solution for the heel section (Fig. 6D) exhibited a truss-like structure that helped reinforce the single point of contact in the keel section (Fig. 5H).
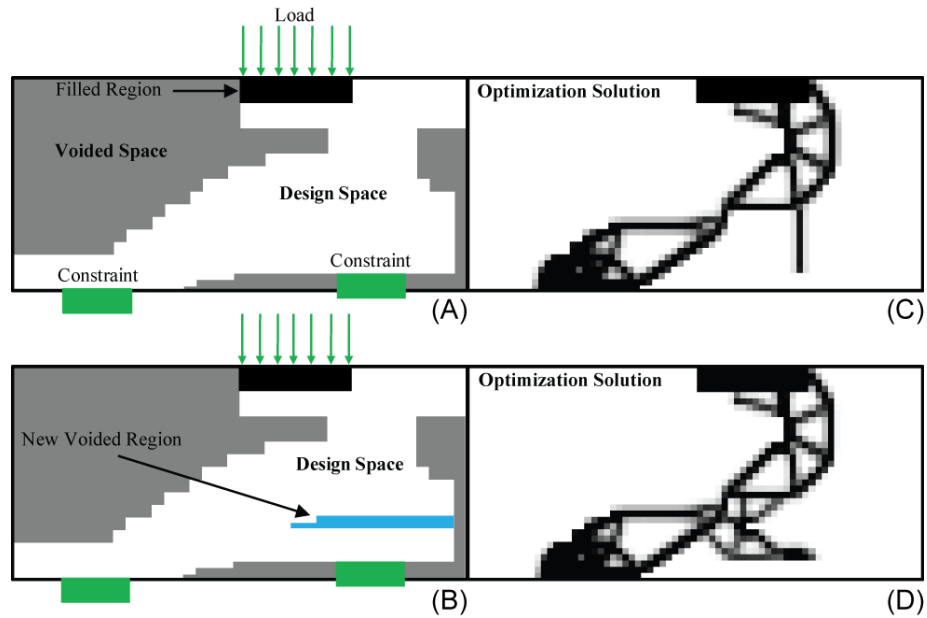

Figure 6. Initial topology optimization solution for the heel section with the fixed keel section (C). A geometric constraint on the allowable design space for the heel (B) was imposed such that the final topology optimization solution (D) did not exhibit a single vertical member.

The topology optimization techniques used in this study reduced the volume (Eq. 2) of the original carbon fiber design (Fig. 4B) by ~16% (Table 1). In addition, the compliance of the topology optimization solution was less than the nominal solution, indicating a stiffer design in foot-flat (Table 1).

Table 1. Compliance and volume values (Eqs. 1, 2) of the final topology optimization solution (Fig. 6D) compared to the nominal carbon fiber shape for the foot flat loading condition (Fig. 4B). The Topology Opt. (Nylon-11/SLS) compliance value represents the change of material conversion from carbon fiber to Nylon-11.

	Nominal Shape (Carbon Fiber)	Topology Opt. (Nylon-11/SLS)
Volume	399.051	332.184
Compliance	6.35E+08	1.17E+07

Solid Model Creation and FEM Validation

The design solution generated via topology optimization (Fig. 6D) was replicated in SolidWorks to create a CAD model of the new foot. The two-dimensional profile was recreated (Fig. 7B), extruded, and cut to match the carbon fiber foot's outer dimensions and critical design features (Fig. 7C).
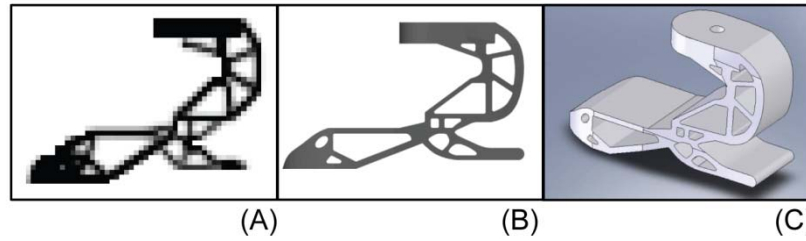
Figure 7. Final topology optimization solution (A) recreated as a sketch in SolidWorks (B) and extruded and cut to match carbon fiber dimensions and critical features (C).

As shown by the FEM results, there were no significant stress concentrations with the design created via topology optimization (Fig. 8.). In addition, the solid model created from the topology optimization used less volume (~35%) than needed by the SLS ESAR design [38] to reproduce the stiffness of the carbon fiber foot (Table 2). Deflection in the foot-flat loading condition of the final design was less than the nominal SLS ESAR design, while the deflections in the toe-only condition were similar (Table 2).
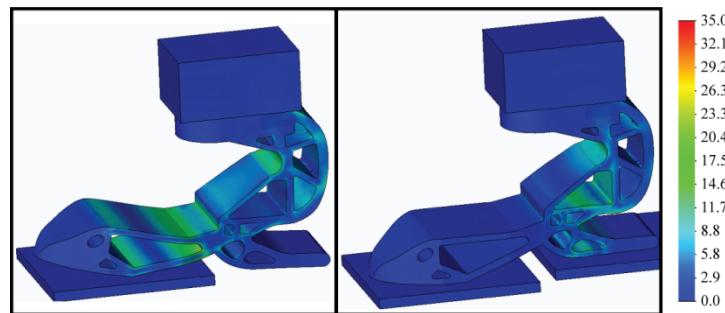

Figure 8. FEM toe-only (left) and foot-flat loading (right) loading conditions von Mises stress plots. Loads applied were 113 and 34 kg for foot-flat and toe-only, respectively. Scale maximum was set to yield strength of Nylon-11 (35 MPa), while scale minimum was set to 0 MPa.

Table 2. FEM displacements for toe-only and foot-flat conditions and volume values of the final design compared to the SLS ESAR foot model [38].

	Displacement (cm)		
	Toe-only	Foot-flat	Volume (cm^3)
SLS ESAR	0.7783	0.8689	377.1
Topology Opt.	1.276	0.2283	244.7

Prototype
   The final design was manufactured successfully using SLS technology (Fig. 9).

Figure 9. Final design prototype manufactured from Nylon-11 using SLS technology.

Discussion

The goal of this study was to develop a framework that uses topology optimization techniques to produce novel prosthetic feet well-suited for SLS fabrication and to validate its use by creating a foot that replicates stiffness characteristics of a commercially available ESAR foot and minimizes material usage.

Justification of Design and Process

The final design satisfies the spatial constraints and will fit inside a shoe. As shown by these results, topology optimization is an effective method for creating new, novel foot geometries suitable for SLS fabrication. The final design represents a material placement strategy unlike any other current prosthetic foot design and can be fabricated without penalty for increased part complexity [42]. The final topology optimization design reduced the material used while increasing stiffness during foot-flat and somewhat decreasing stiffness in toe-only. Due to the reduced volume, the final design weighs less, which may have implications for reducing metabolic cost of amputees [e.g., 43].

Topology Optimization

The geometric constraints implemented in this study greatly affected solutions generated (Figs. 5, 6) and showed promise for improving the practicality of solutions generated via topology optimization. The current topology optimization framework found a compromise solution between the two objectives of minimizing volume (material usage) and matching a targeted compliance. The final solution reduced volume, while compliance in the two loading conditions did not exactly match the target (Table 2). This result is consistent with balancing the two objectives formulated in this framework. However, matching a targeted compliance is more fundamentally important and determines the amount of support provided during amputee gait. In the current design, the larger toe-only displacement (Table 2) coupled with the reduced cross-section in the middle of keel section is an area of concern and could represent a possible fatigue problem. At present, topology optimization techniques are most commonly used as a concept generation tool, intended to provide general layout suggestions. The concepts generated are usually refined with FEM and/or additional parametric optimization. Thus, reformulation of the objective function, constraints, or design space should be made to more closely reproduce the targeted loading response, and a new design prototype should be built and tested to verify its response experimentally.

616

Future Work

Refinement of the toe section should be made. While the keel and heel shape are realistic and practical, the toe section is shorter than the nominal carbon fiber foot shape. The longer curved toe section present in the carbon fiber shape (Figs. 4A) performs an additional task of providing the proper "roll-over" shape during toe-off at the end of the stance. Additional filled material constraints (similar to Fig. 5D) beyond the toe contact with the ground can be easily implemented and not greatly affect loading response in toe-only and foot-flat conditions. We expect that the added material in the toe region would be minimal such that the resulting volume would remain less than the volume of the SLS ESAR foot. A possible foot redesign that incorporates a toe and reinforces the middle of the keel section while still maintaining the critical features generated by the current topology optimization framework is shown (Fig. 10).
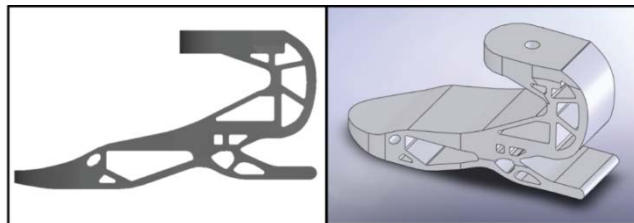

Figure 10. Possible future redesign that includes a toe region to provide the proper roll-over shape and support at toe-off, while reinforcing the middle keel section to reduce deflection in the toe-only loading configuration.

This topology optimization framework was designed to be sequential. First, the keel section geometry was optimized in the toe-only loading condition. Then, the keel section was fixed and the heel section was optimized in a foot-flat condition. A parallel method that takes into account both optimizations of the keel and heel sections at the same time in toe-only and foot-flat conditions may converge on a different solution. A parallel method in this framework could be implemented in the cost function to minimize the differences in compliance during both loading conditions while also minimizing volume.

Closing

This study presents a framework using topology optimization methods to develop new prosthetic feet. The framework was used to generate a prosthetic foot that minimized material usage and attempted to replicate the stiffness characteristics of a commercially available foot. The final solution was validated using FEM to verify the foot's loading response and a prototype was produced. This framework produced a novel foot design, well-suited for SLS fabrication, which with future design modifications has the potential to improve amputee gait by providing energy storage and return and reducing prosthetic weight.

References
1.   Ziegler-Graham, K., et al., *Estimating the prevalence of limb loss in the United States: 2005 to 2050.* Arch Phys Med Rehabil, 2008. **89**(3): p. 422-9.
2.   Lehmann, J.F., et al., *Mass and mass distribution of below-knee prostheses: effect on gait efficacy and self-selected walking speed.* Arch Phys Med Rehabil, 1998. **79**(2): p. 162-8.

3.   Vrieling, A.H., et al., *Gait initiation in lower limb amputees.* Gait Posture, 2008. **27**(3): p. 423-30.

4.   Sanderson, D.J. and P.E. Martin, *Lower extremity kinematic and kinetic adaptations in unilateral below-knee amputees during walking.* Gait Posture, 1997. **6**: p. 126-136.

5.   Nolan, L., et al., *Adjustments in gait symmetry with walking speed in trans-femoral and trans-tibial amputees.* Gait Posture, 2003. **17**(2): p. 142-51.

6.   Silverman, A.K., et al., *Compensatory mechanisms in below-knee amputee gait in response to increasing steady-state walking speeds.* Gait and Posture, 2008.

7.   Czerniecki, J.M., *Rehabilitation in limb deficiency. 1. Gait and motion analysis.* Arch Phys Med Rehabil, 1996. **77**(3 Suppl): p. S3-8.

8.   Burke, M.J., V. Roman, and V. Wright, *Bone and joint changes in lower limb amputees.* Ann Rheum Dis, 1978. **37**(3): p. 252-4.

9.   Melzer, I., M. Yekutiel, and S. Sukenik, *Comparative study of osteoarthritis of the contralateral knee joint of male amputees who do and do not play volleyball.* J Rheumatol, 2001. **28**(1): p. 169-72.

10.   Gitter, A., J.M. Czerniecki, and D.M. DeGroot, *Biomechanical analysis of the influence of prosthetic feet on below-knee amputee walking.* Am J Phys Med Rehabil, 1991. **70**(3): p. 142-8.

11.   Powers, C.M., S. Rao, and J. Perry, *Knee kinetics in trans-tibial amputee gait.* Gait Posture, 1998. **8**(1): p. 1-7.

12.   Bateni, H. and S.J. Olney, *Kinematic and Kinetic Variations of Below-Knee Amputee Gait.* J Prosthet Orthot, 2002. **14**: p. 2-10.

13.   Beyaert, C., et al., *Compensatory mechanism involving the knee joint of the intact limb during gait in unilateral below-knee amputees.* Gait Posture, 2008.

14.   Nolan, L. and A. Lees, *The functional demands on the intact limb during walking for active trans-femoral and trans-tibial amputees.* Prosthet Orthot Int, 2000. **24**(2): p. 117-25.

15.   Winter, D.A. and S.E. Sienko, *Biomechanics of below-knee amputee gait.* J Biomech, 1988. **21**(5): p. 361-7.

16.   Klute, G.K., C.F. Kallfelz, and J.M. Czerniecki, *Mechanical properties of prosthetic limbs: adapting to the patient.* J Rehabil Res Dev, 2001. **38**(3): p. 299-307.

17.   Fey, N.P., A.K. Silverman, and R.R. Neptune, *The influence of increasing steady-state walking speed on muscle activity in below-knee amputees.* J Electromyogr Kinesiol, 2009.

18.   Kulkarni, J., et al., *Chronic low back pain in traumatic lower limb amputees.* Clin Rehabil, 2005. **19**(1): p. 81-6.

19.   Ephraim, P.L., et al., *Phantom pain, residual limb pain, and back pain in amputees: results of a national survey.* Arch Phys Med Rehabil, 2005. **86**(10): p. 1910-9.

20.   Smith, D.G., et al., *Phantom limb, residual limb, and back pain after lower extremity amputations.* Clin Orthop Relat Res, 1999(361): p. 29-38.

21.   Robinson, J.L., G.L. Smidt, and J.S. Arora, *Accelerographic, temporal, and distance gait factors in below-knee amputees.* Phys Ther, 1977. **57**(8): p. 898-904.

22.   Hermodsson, Y., et al., *Gait in male trans-tibial amputees: a comparative study with healthy subjects in relation to walking speed.* Prosthet Orthot Int, 1994. **18**(2): p. 68-77.

23.   Perry, J., et al., *Prosthetic weight acceptance mechanics in transtibial amputees wearing the Single Axis, Seattle Lite, and Flex Foot.* IEEE Trans Rehabil Eng, 1997. **5**(4): p. 283-9.

24.   Hafner, B.J., et al., *Energy storage and return prostheses: does patient perception correlate with biomechanical analysis?* Clin Biomech (Bristol, Avon), 2002. **17**(5): p. 325-44.

25.   Hafner, B.J., et al., *Transtibial energy-storage-and-return prosthetic devices: a review of energy concepts and a proposed nomenclature.* J Rehabil Res Dev, 2002. **39**(1): p. 1-11.

26.   Neptune, R.R., S.A. Kautz, and F.E. Zajac, *Contributions of the individual ankle plantar flexors to support, forward progression and swing initiation during walking.* J Biomech, 2001. **34**(11): p. 1387-98.

27.   Faustini, M.C., et al., *Design and analysis of orthogonally compliant features for local contact pressure relief in transtibial prostheses.* J Biomech Eng, 2005. **127**(6): p. 946-51.

28.   Faustini, M.C., R.R. Neptune, and R.H. Crawford, *The quasi-static response of compliant prosthetic sockets for transtibial amputees using finite element methods.* Med Eng Phys, 2006. **28**(2): p. 114-21.

29.   Faustini, M.C., et al., *An experimental and theoretical framework for manufacturing prosthetic sockets for transtibial amputees.* IEEE Trans Neural Syst Rehabil Eng, 2006. **14**(3): p. 304-10.

30.   Faustini, M.C., et al., *Manufacture of Passive Dynamic ankle-foot orthoses using selective laser sintering.* IEEE Trans Biomed Eng, 2008. **55**(2): p. 784-90.

31.   Rogers, B., et al., *Advanced trans-tibial socket fabrication using selective laser sintering.* Prosthet Orthot Int, 2007. **31**(1): p. 88-100.

32.   Sigmund, O., *On the Design of Compliant Mechanisms using Topology Optimization.* Mechanics Based Design of Structures and Machines, 1997. **25**(4): p. 493 - 524.

33.   Eschenauer, H.A. and N. Olhoff, *Topology Optimization of Continuum Structures: A Review.* Applied Mechanics Reviews, 2001. **54**(4): p. 331-389.

34.   Ohsaki, M. and C.C. Swan, *Topology and Geometry Optimization of Trusses and Frames*, in *Recent Advances in Optimal Structural Design*, S.A. Burns, Editor. 2002, American Society of Civil Engineers: Reston, VA.

35.   Soto, C., *Structural Topology Optimization: From Minimizing Compliance to Maximizing Energy Absorption.* International Journal of Vehicle Design, 2001. **25**(1/2): p. 142-160.

36.   Lin, C.Y., N. Kikuchi, and S.J. Hollister, *A novel method for biomaterial scaffold internal architecture design to match bone elastic properties with desired porosity.* J Biomech, 2004. **37**(5): p. 623-36.

37.   Xinghua, Z., G. He, and G. Bingzhao, *The application of topology optimization on the quantitative description of the external shape of bone structure.* J Biomech, 2005. **38**(8): p. 1612-20.

38.   South, B.J., *Energy Storage and Return Prosthetic Foot Fabrication Using Selective Laser Sintering.* The University of Texas at Austin, Department of Mechanical Engineering, 2008(Master of Science in Engineering Thesis).

39.   Sigmund, O., *A 99 line topology optimization code written in Matlab.* Structural and Multidisciplinary Optimization, 2001. **21**(2): p. 120-127.

40.   Svanberg, K., *The method of moving asymptotes - a new method for structural optimization.* International Journal for Numerical Methods in Engineering, 1987. **24**: p. 359-373.

41.   Hexel.com, *Carbon Fiber Data Sheets.* http://www.hexcel.com/Products/Downloads/Carbon+Fiber+Data+Sheets.htm?ds=Continuous, 2008.

42.   Beaman, J.J., *Solid freeform fabrication: a new direction in manufacturing: with research and applications in thermal laser processing.* 1997.

43.   Browning, R.C., et al., *The effects of adding mass to the legs on the energetics and biomechanics of walking.* Med Sci Sports Exerc, 2007. **39**(3): p. 515-25.